How to cite: *Angew. Chem. Int. Ed.* **2023**, *62*, e202302858
doi.org/10.1002/anie.202302858

Aptamers Hot Paper

Switchable Fluorescent Light-Up Aptamers Based on Riboswitch Architectures

*Tianhe Wang and Friedrich C. Simmel**

Abstract: Fluorescent light-up RNA aptamers (FLAPs) such as Spinach or Mango can bind small fluorogens and activate their fluorescence. Here, we adopt a switching mechanism otherwise found in riboswitches and use it to engineer switchable FLAPs that can be activated or repressed by trigger oligonucleotides or small metabolites. The fluorophore binding pocket of the FLAPs comprises guanine (G) quadruplexes, whose critical nucleotides can be sequestered by corresponding anti-FLAP sequences, leading to an inactive conformation and thus preventing association with the fluorophore. We modified the FLAPs with designed toehold hairpins that carry either an anti-FLAP or an anti-anti-FLAP sequence within the loop region. The addition of an input RNA molecule triggers a toehold-mediated strand invasion process that refolds the FLAP into an active or inactive configuration. Several of our designs display close-to-zero leak signals and correspondingly high ON/OFF fluorescence ratios. We also modified purine aptamers to sequester a partial anti-FLAP or an anti-anti-FLAP sequence to control the formation of the fluorogen-binding conformation, resulting in FLAPs whose fluorescence is activated or deactivated in the presence of guanine or adenine. We demonstrate that switching modules can be easily combined to generate FLAPs whose fluorescence depends on several inputs with different types of input logic.

Introduction

Biomolecular fluorescent reporters are powerful tools with a wide range of applications in cell biology, molecular biology, and biomedicine. Over the past decades, in particular the green fluorescent protein (GFP) and its derivatives have been broadly utilized in bio-labeling and imaging,[1] biosensing,[2] the exploration of signaling pathways[3] and the characterization of gene circuits.[4] With the recent development of RNA-based fluorescent light-up aptamers (FLAPs) such as Spinach,[5] Mango,[6] Corn,[7] RhoBAST,[8] and others,[9] the scope of fluorescent reporters has been considerably widened. The Spinach aptamer can bind the small fluorogen DFHBI (3,5-difluoro-4-hydroxybenzylidene imidazolinone) and thereby increase its fluorescence quantum yield by roughly thousandfold (with an emission wavelength of $\lambda_{em}=501$ nm), while Mango binds to the thiazole-orange derived TO1-biotin fluorogen, leading to a similar increase in fluorescence at $\lambda_{em}=535$ nm. Compared to fluorescent proteins, FLAPs only need to be transcribed from a DNA template and do not require translation or maturation, which makes their dynamics potentially much faster. As functional RNA molecules, they are ideally suited for applications in RNA sensing or as readouts for RNA-based gene circuits. However, they typically suffer from a lower stability and signal intensity in vivo.

Based on crystallographic studies,[10] FLAPs such as Spinach, Mango or Corn all share three basic structial motifs: i) two G-quadruplex platforms, ii) a triplex lid, and iii) an in-plane guanine, which together assemble a binding pocket for the fluorogen[9] (Figure 1d). In addition, a potassium ion is required to stabilize each G-quadruplex. The fluorogen is bound to the binding pocket through non-covalent interactions between its functional groups and the RNA residues. Given the importance of the G-quadruplex motif for the FLAPs, various studies previously attempted to develop switchable FLAPs as biosensors by controlling the folding of the G-quadruplex and the overall fluorogen-binding conformation. For instance, FLAPs can be designed as fusion aptamers (Figure S1), combined with other sensor units such as RNA aptamers,[11] riboswitches,[12] reverse complementary sequences[13] and antigens,[14] and coupled to in situ amplification methods such as the hairpin chain reaction.[15] Upon binding to their cognate targets (small metabolites, RNA, proteins), a structural rearrangement is induced that brings the FLAPs into the stabilized fluorogen-binding conformation. Following a different strategy, folding of split-FLAPs into a fluorescently active conformation can also be facilitated by ligand binding.[16]

In the present work, we sought to utilize switching mechanisms derived from naturally occurring riboswitches to develop FLAPs from fluorogenic aptamers such as Spinach and Mango that can be switched using short RNA triggers and small metabolites (adenine and guanine) as inputs. Riboswitches are functional RNA elements present

[*] T. Wang, Prof. Dr. F. C. Simmel
Physics of Synthetic Biological Systems—E14, Department of Bioscience, TUM School of Natural Science, Technische Universität München
Am Coulombwall 4a, 85748 Garching (Germany)
E-mail: simmel@tum.de

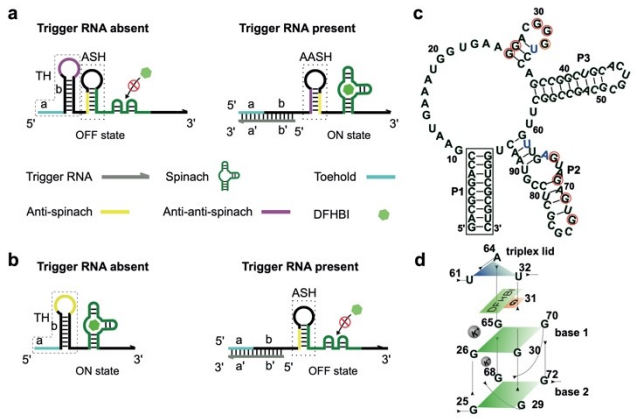

Figure 1. Overview of fluorescent light-up aptamers switched by RNA inputs via toehold-mediated strand invasion. a) Scheme of the switching process of a toehold-Spinach activator. The activator comprises a toehold hairpin (TH) and an anti-Spinach hairpin (ASH), which prevents folding of the Spinach aptamer into an active conformation. In the presence of trigger RNA, an anti-anti-Spinach hairpin (AASH) is formed, and Spinach can fold correctly. b) Conversely, a toehold-Spinach repressor comprises a toehold hairpin and a Spinach aptamer. In the presence of trigger RNA, an ASH is formed, preventing formation of the Spinach aptamer. c) Secondary structure of the Spinach aptamer. Red circles indicate critical guanines involved in G-quadruplex formation, while blue letters indicate nucleotides involved in triplex lid formation. The box marks the lower stem of the aptamer. d) Schematic image of the binding pocket highlighting G-quadruplexes and triplex lid, bases are numbered as in (c).

in the 5′ untranslated region (UTR) of mRNAs, where they regulate downstream gene expression based on the interaction with small metabolites.[17] They are composed of two functional domains—the metabolite-binding domain (an RNA aptamer structure) and the "expression platform", which can switch between two alternative conformations in the free and metabolite-bound states.[18] For instance, in a translational "ON switch", in the ligand-free state of the riboswitch the ribosome binding site (RBS) is base-paired with an anti-RBS sequence in the expression platform, thus preventing translational initiation by the ribosome and translation starting at the start codon AUG. Upon ligand-binding, the aptamer domain undergoes a conformational change, which results in the sequestration of the anti-RBS sequence by an anti-anti-RBS, making the RBS and start codon accessible to the ribosome, and thus activating protein expression from the downstream open reading frame (Figure S2). We adopted this switching principle to realize FLAPs, in which the folding of the FLAP aptamer is controlled by the presence of an adjacent anti-FLAP sequence. We found that anti-FLAP sequences that sequester the critical guanine nucleotides of the FLAPs can prevent the folding of the fluorogen-binding conformation very efficiently, resulting in an extremely low leak signal and thus a very high dynamic range. In the case of ON-switchable FLAPs, an anti-anti-FLAP sequence is initially sequestered in an alternative secondary structure. Refolding of the structure can be promoted by an RNA trigger molecule, which releases the anti-anti-FLAP through a toehold-mediated strand displacement (TMSD) process[19] similar as in gene regulatory toehold switches.[20] Upon refolding, the anti-FLAP sequence is bound by the anti-anti-FLAP, allowing the FLAP to fold into its fluorogen-binding conformation. Alternatively, the anti-FLAP sequence can be hidden within the secondary structure of a purine aptamer,[21,22] which allows to activate the FLAP by the presence of either adenine or guanine. OFF-switchable FLAPs are designed accordingly by initially sequestering the anti-FLAP sequence, and releasing it upon RNA or ligand binding. In our experimental setting, the FLAPs are transcribed from their corresponding gene templates in the absence or presence of triggers, and fluorescence is monitored during in vitro transcription (IVT). We also demonstrate switchable FLAPs with two-input logic, whose fluorescence output depends on the presence of two different triggers. Several of our designs of RNA switchable FLAPs display essentially zero intrinsic leak and can be switched by freely choosable input RNAs, and are thus well-suited to act as reporters for in vitro RNA circuits and nucleic acid amplification schemes.

Results and Discussion

RNA-switchable FLAPs based on TMSD

Our initial goal was to engineer switchable FLAPs with high ON/OFF signal ratios that are activated through binding to small trigger RNAs. To this end, we designed switchable toehold aptamers by augmenting the original FLAP with a toehold hairpin (TH) at its 5′ end containing a 14 nt long, single-stranded toehold region and a 16 bp long stem (Figure 1). Inspired by the structure of riboswitches, we placed a regulatory sequence within the loop region of the toehold hairpin, which was designed to interact with a specific downstream sequence. The designs of the switchable Spinach and Mango aptamers are completely analogous, and we here first focus on the Spinach aptamer. In the case of the Spinach activator (Figure 1a, Figure S3), in the absence of a trigger RNA the toehold hairpin sequesters an anti-anti-Spinach (AAS) domain (generally, an "anti-anti-FLAP" domain), while an anti-Spinach (AS) sequence base-pairs with critical nucleotides of the Spinach aptamer to form the stem of the anti-Spinach hairpin (ASH). For the design of the FLAP sequences, we adjusted the folding free energies of critical secondary structural elements using the nucleic acid analysis tool NUPACK.[23] The folding free energy of the ASH (ΔG_{ASH}) is designed to be lower than the free energy of the lower stem P1 of the Spinach aptamer ($\Delta G_{\mathrm{Spinach\text{-}P1}} = -17.48\ \mathrm{kcal\,mol^{-1}}$). In the absence of trigger, the formation of the G-quadruplexes and thus binding of DFHBI is disabled (OFF state). In the presence of trigger RNA, the toehold hairpin is opened via TMSD, releasing the AAS sequence, which can base-pair with the AS sequence and thus form a stable anti-anti-Spinach hairpin (AASH). The free energy of the AASH (ΔG_{AASH}) is chosen intermediate between the free energies of ASH and TH ($\Delta G_{\mathrm{TH}} < \Delta G_{\mathrm{AASH}} < \Delta G_{\mathrm{ASH}}$). The conformational rearrange-

ment restores the G-quadruplexes, which facilitates binding of the DFHBI fluorogen and thus activates fluorescence (ON state). We also designed toehold-Spinach repressors (Figure 1b), which use a similar switching process to inhibit the formation of the binding pocket for the fluorogen. In this case, the TH loop is used to sequester the anti-Spinach sequence. In the absence of trigger RNA, the Spinach aptamer correctly folds. In the presence of trigger RNA, the TH is unfolded, releasing the AS, which in turn leads to the formation of the anti-Spinach hairpin and thus inhibition of fluorogen binding (OFF state).

To fine-tune the switching behavior of the toehold-Spinach activators, we designed and tested five different AS sequences that sequester different sub-sets of the nine critical guanine nucleotides of the Spinach aptamer (Figure 2a). In order to assess their performance, we transcribed both switch RNA and trigger RNA in the presence of 20 μM of fluorogen using the same DNA template concentration (10 nM) using an IVT mix (cf. Experimental Section and Supporting Information) and simultaneously measured the fluorescence signal. Anti-Spinach sequence #1 can base-pair with the first eleven nucleotides of the lower stem sequence of the Spinach aptamer (in this case none of the critical guanines is targeted), while anti-Spinach #2 and #3 target the loop region of the Spinach aptamer (nucleotides 10 to 34), including 5 critical guanines and a uracil that participate in the formation of the G-quadruplex bases and the triplex lid (cf. Figure 1d). In addition, anti-Spinach #4 and #5 can bind to the critical nucleotides in the range from 61 to 86, which is close to the 3′ end of the aptamer. As shown in Figure 2a, in the OFF state—in the absence of trigger—fluorescence is tightly suppressed for all versions. Notably, for guanine-sequestering versions #2, #3, #4 and #5 the signal is indistinguishable from the fluorescence of a blank measurement containing only transcription mix and DFHBI. Among these versions, #3 provided the highest ON signal in the presence of trigger RNA, corresponding to an ON/OFF ratio of ≈22 under the conditions of this co-transcriptional experiment. FLAP #3 sequesters all three critical guanines on the 5′ side of the Spinach aptamer, which appears to be favorable for refolding upon activation. FLAP #4, sequestering four guanines closer to the 3′ end of Spinach appears to be less performant in comparison. This may be attributed to the larger distance between the anti-anti-Spinach sequence in the TH at the 5′ end and the ASH. We also studied the switching behavior of FLAP #3 using other experimental settings, either by co-transcribing switch and trigger RNA or using purified RNA components, and found ON/OFF ratios ranging between 20 and over 200 (Figure S4, note that the theoretical maximum would be ≈1000, which is given by the increase in quantum yield when DFHBI binds to Spinach[9]), indicating that experimental conditions can be further optimized for sensor applications.

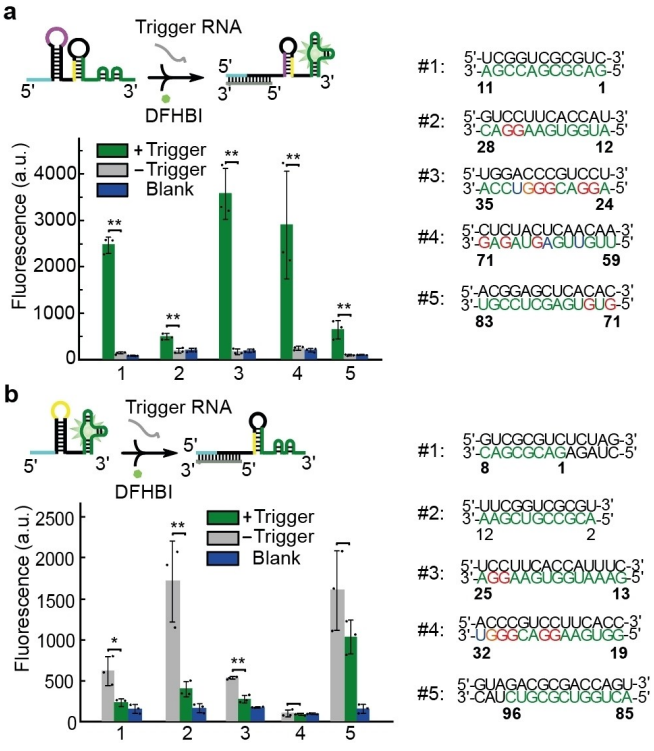

Figure 2. Relative fluorescence intensities obtained from different toehold-Spinach activators (a) and repressors (b) that utilize different anti-Spinach sequences in the presence or absence of trigger RNA, respectively. Sequestered critical guanine nucleotides of the Spinach aptamer are highlighted in red (cf. Figure 1c). The heights of the bars are obtained as the mean of three independent replicates, the error bars represent their standard deviation (s.d.). In a), activators #3 and #5 displayed zero fluorescence above background in the absence of trigger RNA, and therefore the ON/OFF ratio was not calculated. The statistical significance of the difference between the trigger RNA+ and the trigger RNA- condition was determined via Welch's t-test, ** indicates a p-value < 0.01.

For the toehold-Spinach repressors, we similarly designed five variants with different AS sequences (Figure 2b). Anti-Spinach #1 and #2 were designed to sequester the sequence of lower stem P1 close to the 5′ end of the Spinach aptamer and thus prevent its folding. Anti-Spinach #1 also includes a part of the linker sequence between the toehold hairpin and the aptamer, and resulted in the highest ON/OFF ratio among the five studied AS sequences. Anti-Spinach #2 also targets the lower stem P1, but exhibits higher leakage in the OFF state than anti-Spinach #1, leading to a lower ON/OFF ratio. Other variants such as anti-Spinach #3 (targeting two critical guanine nucleotides) and anti-Spinach #5 (targeting the 3′ end of lower stem P1) resulted in lower ON/OFF ratios or, as in the case of anti-Spinach #4 (targeting five guanines), did not perform at all. The reduced performance of the repressors compared to the activators is expected and is similar as observed for riboregulator switches. Whereas the activators will always have a very low OFF state due to the co-transcriptional sequestration of a critical subsequence of the fluorogenic aptamer, repressors initially fold into an active fluorescent state, unless they are de-activated by trigger RNA co-transcriptionally. The latter process is expected to be inefficient, however, for typical RNA trigger concentrations, and thus a considerable leak signal is unavoidable.

We analogously applied our design approach to the Mango aptamer[6] which also folds into a G-quadruplex

topology, in which it binds to its specific fluorogen TO1-biotin (Figure S5). As for the Spinach aptamer, we designed five toehold-Mango activators comprising different anti-Mango (AM) sequences to target sub-sequences of the mango aptamer (Figure S6). In contrast to the Spinach aptamer, AM variants #1 and #5 that sequestered the stem of the Mango aptamer close to the 5′ or 3′ end performed better than those variants (#2–#4) targeting the loop region containing the critical nucleotides. We also designed five variants of a toehold-Mango aptamer repressor, of which again only those targeting the Mango stem (#1, #5) resulted in switching. The RNA-switchable Mango aptamers generally performed less than the Spinach versions, which we attribute to the lower K_D for the complex of Mango with TO1-biotin ($\approx$3 nM) compared with the Spinach-DFHBI complex ($\approx$300 nM),[9] presumably leading to a higher leak signal in the OFF state.

Switchable FLAPs based on purine aptamers

Purine aptamers consist of a three-way junction structure in which three stems (P1–P3, cf. Figure 3c) surround a central core that contains several critical nucleotides for ligand binding.[21b,24] The P2 and P3 stems can interact via long-range loop-loop interactions even in the absence of ligand, which along with the core forms a preorganized binding pocket that enables rapid ligand binding (Figure 3d).[22]

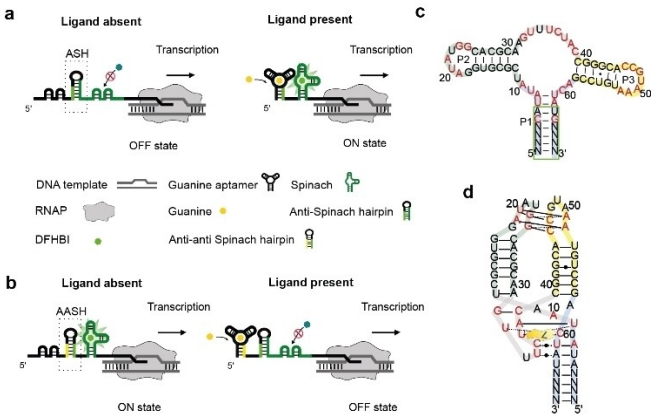

Figure 3. Guanine-dependent Spinach switches. a) Scheme of the switching process for the guanine-Spinach activator. In the OFF state, critical nucleotides of the Spinach aptamer are sequestered in the anti-Spinach hairpin (ASH). In the presence of guanine, the binding pocket of the guanine aptamer is stabilized and the anti-Spinach sequence is sequestered in its P1 stem. Hence, the Spinach aptamer can fold, bind to DFHBI and activate its fluorescence. The transcription process is also indicated as its kinetics determines the time window during which the ligand can bind, which is given by the time between the formation of the guanine binding pocket (see panels (c) & (d)) and the formation of the anti-spinach hairpin. b) In the guanine-Spinach repressor, in the absence of guanine the anti-Spinach sequence is bound in the anti-anti-Spinach hairpin (AASH). In the presence of guanine, the AS sequence sequesters critical nucleotides of the Spinach aptamer and thus de-activates it. As in panel a), binding of guanine is assumed to occur co-transcriptionally. c) Secondary structure of the guanine aptamer with the P1, P2 and P3 stems indicated. Nucleotides critical for the function of the aptamer are colored in red. The "N" nucleotides in the P1 stem (highlighted in the green box) were varied for the design of the guanine-switchable FLAPs. d) Scheme of the tertiary structure of the guanine ligand binding pocket involving loop-loop interaction between the P2 and P3 stems.

In the context of a riboswitch, once the aptamer binds its ligand, quadruplex interactions within the central core and the P1 stem are further stabilized, preventing the disassembly of the aptamer and rearranging the secondary structure of the downstream sequence. In this work, we modified the P1 stem of the guanine and adenine aptamers to achieve switching of FLAPs in the presence of purines (Figure 3a & b, Figure S7). The stability of the P1 stem affects the free energy of formation of the ligand-binding pocket. We therefore designed a series of structures, in which the P1 stem was modified to contain different AS or AAS sequences, each comprising six bases complementary to specific downstream sequences. The critical nucleotides of the guanine or adenine aptamers that participate in loop-loop interaction and binding pocket formation were left untouched. In the case of the guanine-Spinach activator (Figure 3a), in the absence of guanine the AS sequence base-pairs with the Spinach aptamer to form a stable ASH, which prevents folding of the Spinach G-quadruplexes and fluorogen binding (OFF state).

To ensure proper switching, the folding free-energy of the ASH was designed to be lower than that of the preorganized, ligand-free guanine aptamer structure ($\Delta G_{(G\text{-free})}$) and of the P1 stem of the Spinach aptamer (i.e., $\Delta G_{ASH} < \Delta G_{(G\text{-free})}$ and $\Delta G_{ASH} < \Delta G_{(spinach\text{-}P1)}$). Upon ligand binding, the guanine aptamer is stabilized ($\Delta G_{(G\text{-bound})} < \Delta G_{ASH}$), suppressing the formation of the ASH and thus activating Spinach folding and fluorescence (ON state). Conversely, in the case of the guanine-Spinach repressors, we inserted an AAS into the P1 stem of the guanine aptamer, which can form a stable AASH and thus —in the absence of guanine— allow the formation of the Spinach G-quadruplexes (ON state). As above, the folding free energy of the AASH is designed to be lower than $\Delta G_{(G\text{-free})}$ and ΔG_{ASH}. Ligand binding stabilizes the aptamer and the AAS sequence is sequestered within its P1 stem, which in turn results in the formation of an anti-Spinach hairpin (OFF state). For all guanine-Spinach switch designs, we utilized the anti-Spinach sequence #1 developed for the toehold-Spinach switches, and fine-tuned the free-energy of the guanine aptamer P1 stem to optimize the switching performance. As shown in Figure 4a, we designed four P1 versions for the guanine-Spinach activators, of which two (#1 and #2) were comprised of 8 bp (resulting in a folding free energy > -10 kcal mol^{-1}), while versions #3 and #4 comprised an additional base-pair in the stem (and a free energy below -10 kcal mol^{-1}). We again tested the guanine-Spinach activators in IVT reactions using ligand concentrations of 20 μM (DFHBI) and 0 μM or 50 μM of guanine, respectively. We found that with co-transcriptional ON/OFF ratios of $\approx$12 and $\approx$23 the short stem versions #1 and #2 performed considerably better than the two other versions, which exhibited relatively high leak signals. The leak is likely caused by the higher stability of the P1 stem in

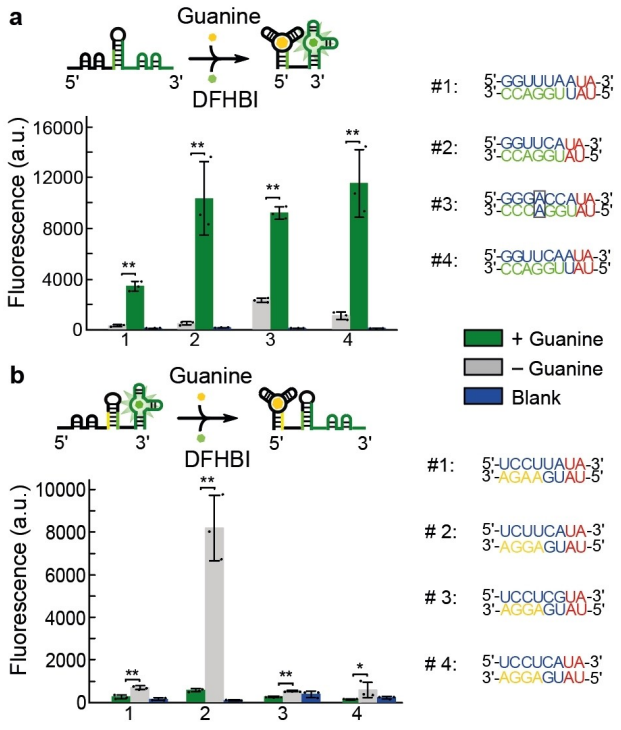

Figure 4. Fluorescence intensities obtained for different versions of guanine-Spinach activators (a) and repressors (b) that utilize different P1 stem sequences in the presence of 0 μM or 50 μM guanine, respectively. Shown are the mean values of for three independent measurements, error bars represent their s.d. (statistical significance of the differences was determined via Welch's t-test, $^{**}p$-value < 0.01). The corresponding P1 sequences are shown on the right. Conserved nucleotides are colored in red, variable nucleotides are shown in blue. Sequestered nucleotides of the Spinach aptamer are shown in green, while anti-Spinach nucleotides are colored yellow. A sequence mismatch on the P1 stem is highlighted with a black box. The blue bars indicate the background level of a blank measurement containing TX mix and DFHBI.

versions #3 and #4, whose formation competes with the folding of the anti-spinach hairpin and might stabilize the active Spinach conformation also in the absence of guanine. In the case of the guanine-Spinach repressors, four design versions with different P1 stem sequence were investigated (Figure 4b). Repressor version #2 with an internal mismatch in the P1 stem performed worst in terms of leak signal in the OFF state, but had the highest fluorescence signal in the ON state, resulting in an ON/OFF ratio of ≈15. All other designs with more stable stems showed a lower leak, but displayed a reduced ON-fluorescence, indicating the mismatch is required to facilitate refolding of the secondary structure.We applied the same design principle to develop ligand-dependent Spinach switches based on an adenine aptamer derived from a riboswitch found in many Gram-positive bacteria,[25] resulting in several performant adenine-sensing activators and repressors (Figure S7).

Logic gate construction by using switchable FLAPs

We next sought to combine several of the toehold- and ligand-controlled FLAPs to create two-input switches with various types of input logic. To this end, we developed a design strategy, in which the folding of the Spinach aptamer structure was influenced by introducing switchable domains at both of its 5′ and 3′ ends.

To achieve AND gate behavior, we combined the Spinach aptamer with two toehold-Spinach activator domains (Figure 5a). Each activator includes an ASH which sequesters critical nucleotides of the Spinach aptamer and prevents folding of its G-quadruplexes. Only in the presence of the two cognate RNA triggers as inputs, each module is activated by TMSD, the G-quadruplexes are restored and fluorescence is activated. Similarly, we also combined two toehold-Spinach repressor modules with the Spinach aptamer to sequester its critical nucleotides either from the 5′ end or 3′ end, resulting in NOR gate behavior (Figure 5b).

Accordingly, the combination of an activator and a repressor module on the same FLAP platform results in a logic NIMPLY (=A AND (NOT B)) gate (Figure 5c). Notably, in this case we observed an appreciable leak signal in the presence of both trigger RNAs, indicating that inhibition by the repressor module at the 3′ end was incomplete. As fluorescence was monitored during in vitro transcription of the switchable FLAP, it is likely that folding of a fraction of the Spinach aptamers was promoted by the activating trigger before the repressing trigger could bind to the repressor module. We also created an AND gate by controlling the Spinach aptamer with both a guanine- and an RNA-dependent activator (Figure 5d). Such or similar gates may play a role in the evaluation of diagnostic rules, which can be formulated as logical expressions, such as the detection of cancer-related miRNA patterns.[26]

In summary, we have successfully developed and characterized switchable fluorescent light-up aptamers (FLAPs), which can be switched using trigger RNAs or purine ligands. Our switchable FLAPs combine structural features of natural riboswitches with the switching mechanism of synthetic riboregulators. This approach allows the realization of both ON and OFF switches with a performance that compares favorably with previously developed switchable Spinach aptamers.[27] In our designs, we inserted a regulatory RNA sequence into the loop region of a toehold hairpin which could be switched by toehold-mediated strand displacement, inducing the formation of a secondary structure in which the fluorogenic aptamer is either activated (for ON switches) or de-activated (OFF switches). Importantly, the sequence of the toehold-region and the stem—and thus the trigger RNA—can be freely chosen and is not constrained by the aptamer sequence itself. In order to demonstrate the modularity and orthogonality of our design, we studied the crosstalk between eight toehold-Spinach activators with orthogonal trigger RNAs. As shown in Figure S8, the switches exhibit highly orthogonal switching behavior, indicating the potential for application in the detection of natural RNA sequences.

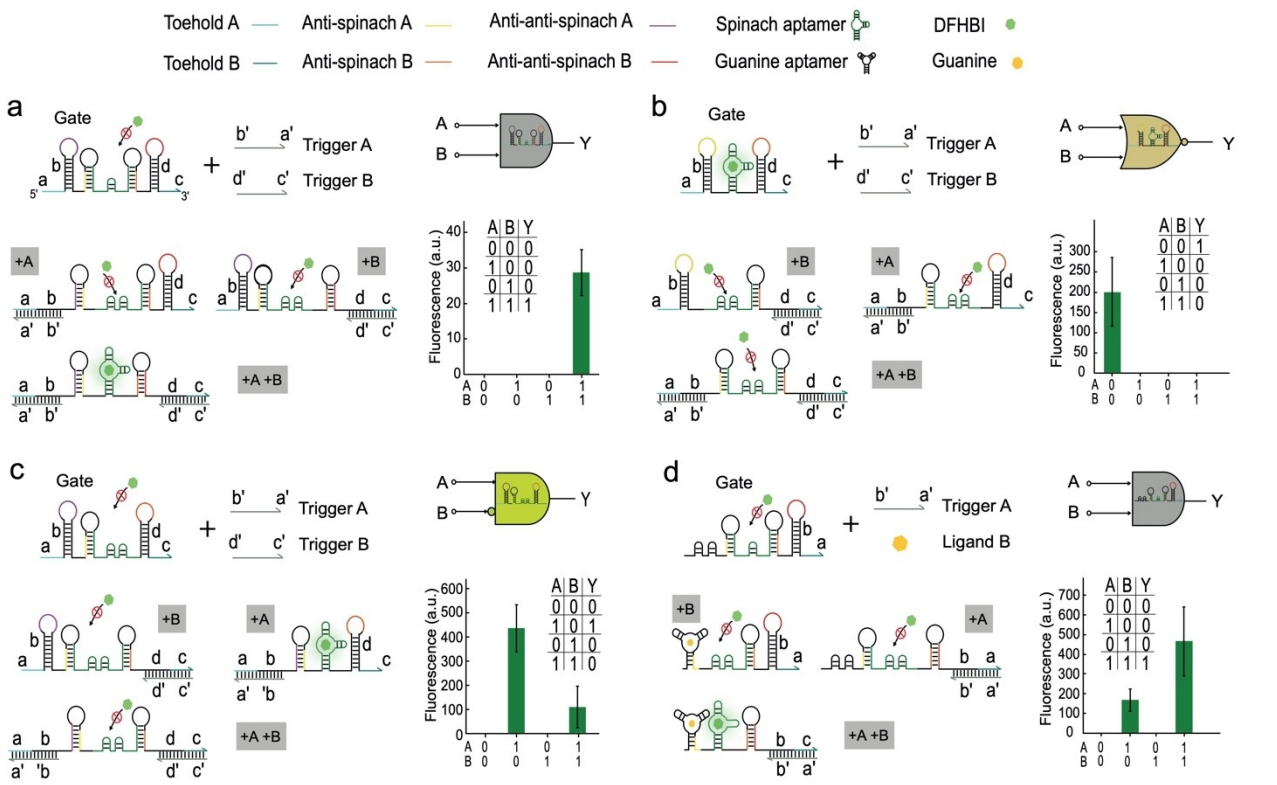

Figure 5. Design and characterization of two-input logic gates based on toehold-Spinach and guanine-Spinach switches. a) A two-input AND gate is realized with two toehold-Spinach activators at the 5′ and 3′ termini of the Spinach aptamer. Each activator module is composed of a toehold hairpin and an ASH. Binding of input Triggers A and B opens their respective toehold hairpins and restores the Spinach aptamer. b) A two-input NOR gate is composed of two toehold-Spinach repressors at its both ends. Binding of either Trigger A or B leads to the disruption of the Spinach aptamer. c) A NIMPLY gate combines an activating and a repressing input module, leading to activation of fluorescence only in the presence of Trigger A as indicated. d) An AND gate with hybrid input composed of a guanine-Spinach activator and a toehold-Spinach activator. The presence of guanine stabilizes the purine aptamer at the 5′ end, while RNA Trigger A leads to a refolding of the structure at the 3′ end, resulting in AND gate input logic as indicated. The fluorescence outputs of all gates are shown as the mean values of background subtracted fluorescence levels for three independent measurements, error bars represent their s.d.

Using a similar strategy, we have also shown that FLAPs can be rendered into riboswitch-inspired aptamer switches, in which the binding of a small molecule ligand influences the formation of the fluorogenic aptamer. In contrast to recent work, in which the adenine riboswitch was re-purposed into an allosteric light-up aptamer using a SELEX approach,[12b] we re-modeled the variable sequences on the P1 stem of the guanine or adenine aptamers into specific AS and AAS sequences, resulting in strong fluorescence suppression in the OFF state and improved ON/OFF ratios. Purine aptamers have a characteristic preorganized ligand-binding structure. Previous studies revealed that several nucleotides contributing to the formation of the ligand-binding site have a major influence on the K_D of ligand binding.[28] Aside from these nucleotides, the free energy of folding of the preorganized structure affects the stability of the ligand-binding site, and thereby influences the refolding process of the downstream structure. We found that when the free energy of the purine aptamer domain of our switch is below $-18.00\,\mathrm{kcal\,mol^{-1}}$, it is capable of sequestering the AS sequence even in the absence of its ligand. We hence fine-tuned the free energy of the P1 stem to influence the refolding of the ASH and the K_D of ligand binding. Interestingly, for both guanine and adenine Spinach switches, the ON/OFF ratios did not have a clear correlation with the free energy of the P1 stem, suggesting a more complex competition between the formation of the ASH and the ligand-binding pocket.

Our design approach also allows for control over the folding of the FLAP using two distinct toehold hairpins attached to the 5′ and 3′ end, resulting in two-input logic control of fluorescence activation by two independent RNA inputs. We also developed a two-input switch that is activated by a small ligand and a trigger RNA, using combination of the guanine-Spinach switch and the toehold-Spinach switch. While the AND gate activators with two RNA inputs displayed almost ideal behavior, logic gates involving repressor modules or guanine as an input were slightly leaky, as would be expected from the behavior of the individual switches. In principle, our general approach should be applicable also to other fluorogenic aptamers containing "critical nucleotides". A potential approach to extend our two-input gates to larger numbers of inputs could be the utilization of multi-arm junctions as input modules, as previously demonstrated for translational toehold riboregulators.[29]

With potential in vivo sensing applications in mind, we also engineered the Broccoli aptamer into a switch, which is known to display greater in vivo stability in bacteria. Such a switch indeed appears to be functional in *E. coli*, albeit with a moderate ON/OFF ratio of ≈4 (Figure S9). To further demonstrate the potential for applications in diagnostic RNA sensing, we also designed FLAPs that respond to RNA sequences derived from the SARS-CoV-2 genome, which were pre-amplified with the isothermal amplification Scheme NASBA[30] (Details in the Supporting Information, Figure S10).

Conclusion

In conclusion, we have demonstrated that the molecular architecture of riboswitches and riboregulators can be adopted to realize switchable fluorescent light-up aptamers which are controlled by one or several RNA or small molecule inputs. The resulting switches show very low OFF signals, which in several cases is indistinguishable from background. Notably, our design allows a complete decoupling of the inputs from the FLAP sequence, which is essential for the realization of sensor or biocomputing applications without any sequence constraints. Some of the features of our switches can be easily understood—e.g., leaky signals in OFF states in cases where the RNA structures are too weak, or the loss of "switchability" in cases, where one of the alternative structures becomes too strong. Nevertheless, rational design of switches for low OFF signals and high dynamic range remains challenging.[31] We anticipate that further optimization of such switchable RNA structures may benefit from recent machine learning approaches,[32] and incorporation of "community-based" knowledge.[33]

Acknowledgements

This work was funded by the Deutsche Forschungsgemeinschaft (DFG, German Research Foundation)—project no. 468955252 and through the DFG Research Training Group "Molecular Principles of Synthetic Biology" GRK 2062—project A3. We gratefully acknowledge support by the European Research Council (project AEDNA, grant number 694410). We appreciate the help of Dr. Sandra Sagredo who provided homemade T7 RNA polymerase for the experiments. Open Access funding enabled and organized by Projekt DEAL.

Conflict of Interest

The authors declare no conflict of interest.

Data Availability Statement

All data is available in the Zenodo repository (https://doi.org/10.5281/zenodo.7836872), or from the authors.

Keywords: Fluorescent Light-up Aptamers · Purine Aptamer · Sensors · Toehold-Mediated Strand Displacement

[1] R. M. Hoffman, *Lab. Invest.* **2015**, *95*, 432–452.
[2] A. J. Meyer, T. Brach, L. Marty, S. Kreye, N. Rouhier, J. P. Jacquot, R. Hell, *Plant J.* **2007**, *52*, 973–986.
[3] E. A. Bach, L. A. Ekas, A. Ayala-Camargo, M. S. Flaherty, H. Lee, N. Perrimon, G.-H. Baeg, *Gene Expression Patterns* **2007**, *7*, 323–331.
[4] T. Steiner, P. Hess, J. H. Bae, B. Wiltschi, L. Moroder, N. Budisa, *PLoS One* **2008**, *3*, e1680.
[5] J. S. Paige, K. Y. Wu, S. R. Jaffrey, *Science* **2011**, *333*, 642–646.
[6] E. V. Dolgosheina, S. C. Jeng, S. S. S. Panchapakesan, R. Cojocaru, P. S. Chen, P. D. Wilson, N. Hawkins, P. A. Wiggins, P. J. Unrau, *ACS Chem. Biol.* **2014**, *9*, 2412–2420.
[7] K. D. Warner, L. Sjekloća, W. Song, G. S. Filonov, S. R. Jaffrey, A. R. Ferré-D′Amaré, *Nat. Chem. Biol.* **2017**, *13*, 1195–1201.
[8] M. Sunbul, J. Lackner, A. Martin, D. Englert, B. Hacene, F. Grün, K. Nienhaus, G. U. Nienhaus, A. Jäschke, *Nat. Biotechnol.* **2021**, *39*, 686–690.
[9] S. Neubacher, S. Hennig, *Angew. Chem. Int. Ed.* **2019**, *58*, 1266–1279.
[10] H. Huang, N. B. Suslov, N.-S. Li, S. A. Shelke, M. E. Evans, Y. Koldobskaya, P. A. Rice, J. A. Piccirilli, *Nat. Chem. Biol.* **2014**, *10*, 686–691.
[11] S. DasGupta, S. A. Shelke, N.-s. Li, J. A. Piccirilli, *Chem. Commun.* **2015**, *51*, 9034–9037.
[12] a) M. You, J. L. Litke, S. R. Jaffrey, *Proc. Natl. Acad. Sci. USA* **2015**, *112*, E2756–E2765; b) S. K. Dey, G. S. Filonov, A. O. Olarerin-George, B. T. Jackson, L. W. S. Finley, S. R. Jaffrey, *Nat. Chem. Biol.* **2022**, *18*, 180–190.
[13] K. Huang, F. Doyle, Z. E. Wurz, S. A. Tenenbaum, R. K. Hammond, J. L. Caplan, B. C. Meyers, *Nucleic Acids Res.* **2017**, *45*, e130.
[14] A. Bertucci, A. Porchetta, F. Ricci, *Anal. Chem.* **2018**, *90*, 1049–1053.
[15] K. Ren, R. Wu, A. P. K. K. K. Mudiyanselage, Q. Yu, B. Zhao, Y. Xie, Y. Bagheri, Q. Tian, M. You, *J. Am. Chem. Soc.* **2020**, *142*, 2968–2974.
[16] R. Soni, D. Sharma, A. M. Krishna, J. Sathiri, A. Sharma, *Org. Biomol. Chem.* **2019**, *17*, 7222–7227.
[17] M. Mandal, R. R. Breaker, *Nat. Rev. Mol. Cell Biol.* **2004**, *5*, 451–463.
[18] A. Roth, R. R. Breaker, *Annu. Rev. Biochem.* **2009**, *78*, 305–334.
[19] a) D. Y. Zhang, G. Seelig, *Nat. Chem.* **2011**, *3*, 103–113; b) F. C. Simmel, B. Yurke, H. R. Singh, *Chem. Rev.* **2019**, *119*, 6326–6369.
[20] A. A. Green, P. A. Silver, J. J. Collins, P. Yin, *Cell* **2014**, *159*, 925–939.
[21] a) S. D. Gilbert, S. J. Mediatore, R. T. Batey, *J. Am. Chem. Soc.* **2006**, *128*, 14214–14215; b) J. N. Kim, R. R. Breaker, *Biol. Cell* **2008**, *100*, 1–11.
[22] O. M. Ottink, S. M. Rampersad, M. Tessari, G. J. Zaman, H. A. Heus, S. S. Wijmenga, *RNA* **2007**, *13*, 2202–2212.
[23] J. N. Zadeh, C. D. Steenberg, J. S. Bois, B. R. Wolfe, M. B. Pierce, A. R. Khan, R. M. Dirks, N. A. Pierce, *J. Comput. Chem.* **2010**, *31*, 170–173.

[24] S. D. Gilbert, C. D. Stoddard, S. J. Wise, R. T. Batey, *J. Mol. Biol.* **2006**, *359*, 754–768.
[25] J.-F. Lemay, J. C. Penedo, R. Tremblay, D. M. Lilley, D. A. Lafontaine, *Chem. Biol.* **2006**, *13*, 857–868.
[26] a) G. A. Calin, C. M. Croce, *Nat. Rev. Cancer* **2006**, *6*, 857–866; b) C. Zhang, Y. Zhao, X. Xu, R. Xu, H. Li, X. Teng, Y. Du, Y. Miao, H. C. Lin, D. Han, *Nat. Nanotechnol.* **2020**, *15*, 709–715.
[27] a) S. Bhadra, A. D. Ellington, *Methods in Enzymology, Vol. 550*, Elsevier, Amsterdam, **2015**, pp. 215–249; b) S. Bhadra, A. D. Ellington, *RNA* **2014**, *20*, 1183–1194.
[28] J. Mulhbacher, D. A. Lafontaine, *Nucleic Acids Res.* **2007**, *35*, 5568–5580.
[29] D. Ma, Y. Li, K. Wu, Z. Yan, A. A. Tang, S. Chaudhary, Z. M. Ticktin, J. Alcantar-Fernandez, J. L. Moreno-Camacho, A. Campos-Romero, A. A. Green, *Nat. Biomed. Eng.* **2022**, *6*, 298–309.
[30] a) J. Compton, *Nature* **1991**, *350*, 91–92; b) K. Pardee, A. A. Green, M. K. Takahashi, D. Braff, G. Lambert, J. W. Lee, T. Ferrante, D. Ma, N. Donghia, M. Fan, N. M. Daringer, I. Bosch, D. M. Dudley, D. H. O'Connor, L. Gehrke, J. J. Collins, *Cell* **2016**, *165*, 1255–1266.
[31] A. Boussebayle, D. Torka, S. Ollivaud, J. Braun, C. Bofill-Bosch, M. Dombrowski, F. Groher, K. Hamacher, B. Suess, *Nucleic Acids Res.* **2019**, *47*, 4883–4895.
[32] A.-C. Groher, S. Jager, C. Schneider, F. Groher, K. Hamacher, B. Suess, *ACS Synth. Biol.* **2019**, *8*, 34–44.
[33] a) J. O. L. Andreasson, M. R. Gotrik, M. J. Wu, H. K. Wayment-Steele, W. Kladwang, F. Portela, R. Wellington-Oguri, E. Participants, R. Das, W. J. Greenleaf, *Proc. Natl. Acad. Sci. USA* **2022**, *119*, e2112979119; b) H. K. Wayment-Steele, W. Kladwang, A. I. Strom, J. Lee, A. Treuille, A. Becka, E. Participants, R. Das, *Nat. Methods* **2022**, *19*, 1234–1242.

Manuscript received: February 24, 2023
Accepted manuscript online: May 10, 2023
Version of record online: June 2, 2023